Supporting Information

Synthesizing Alkynyl-Decorated 2D conjugated Nonfullerene Acceptors for Efficient Polymer Solar Cells

Zhongfei Liu[#a,c], Wanru Liu[#a,b,c], Dan Su[#b,c], Fugang Shen[b], Shuying Huo[b], Mingmei Han[a], Aiju Xu*[a], Chuanlang Zhan*[a,c]

[a] Key Laboratory of Excitonic Materials Chemistry and Devices (EMC&D) and Key Laboratory of Green Catalysis, College of Chemistry and Environmental Science, Inner Mongolia Normal University, Huhhot 010022, China

E-mail: clzhan@imnu.edu.cn (C.Z.), ORCID iD 0000-0001-5127-0973 (C.Z.).

xuaj@imnu.edu.cn (A.X.)

[b] College of Chemistry and Environmental Science, Hebei University, Baoding 071002, Hebei province, China

[c] Beijing National Laboratory for Molecular Sciences, CAS Key Laboratory of Photochemistry, Institute of Chemistry, Chinese Academy of Sciences, Beijing 100190, China.

1. General information

The materials of PEDOT:PSS, PDINO, PM6 and end groups (IC-2F and IC-2Cl) were purchased from Solarmer company. The intermediate ASiBDT-Sn and TT were purchased from Hyper Inc. ^{1}H NMR and ^{13}C NMR spectra were measured with Bruker Fourier 300 and Bruker AvancIII 400HD spectrometers. UV-vis absorption spectra were recorded on a SHIMADZU UV-2600 spectrophotometer. Cyclic voltammetry curves were measured by CHI660E electrochemical workstation at a scan rate of 50 mV/s using tetrabutylammonium tetrafluoroborate (Bu_4NBF_4) as the supporting electrolyte, Ag/AgCl as the reference electrode, platinum wire as the counter electrode, and platinum plate as the working electrode. The external quantum efficiency (EQE) spectra were measured by Enli Technology Co. Ltd. QE-R3011instrument. The *J-V* curves were measured through the Keithley 2400 Source-Measure Unit in high purity N_2-filled glove box. The atomic force microscopy (AFM) height images were studied by Bruker multimode 8. The transimission electron microscopy (TEM) images were measured by JEM-2100F operated at 200 kV. The charge mobilities (μ_e and μ_h) were measured through the space charge limited current (SCLC) method. The thickness of the solid films was measured using a Dektak Profilometer. GIWAXS data were carried out with a Xeuss 2.0 SAXS/WAXS laboratory beamline using a Cu X-ray source (8.05 keV, 1.54 Å) and Pilatus3R 300K detector. The incidence angle is 0.2°.

2. Fabrication of organic solar cells (OSCs)

OSCs were fabricated with a traditional device structure of ITO /PEDOT: PSS/PDINO/Al. ITO coated glass substrates were pre-cleaned with deionized water, CMOS grade acetone and isopropanol in turn for 15 min, followed by treating with UV-ozone for 0.5 h. Atop the cleaned ITO surface a PEDOT:PSS layer (~20 nm) was coated and dried at 150 °C for 15 min. The mixture of PM6 and acceptors in a fixed weight ratio was dissolved in chloroform (CF) with a concentration of 16 mg/mL and stirring the active layer solution for 4 h at room temperature. Different ratios of 1-CN (1-chloronaphthalene) were added to the solution before device fabrication. The blend solution were spin-coated on the top of PEDOT:PSS layer followed by a thermal annealing step (100 °C, 10 min). The optimal thickness of the binary and ternary BHJ film was about 100 nm. Atop the active layer, the electron transporting layer of PDINO was spin-coated. The concentration was 1 mg/mL. The optimal rotating speed was 2000-3000 rpm. Finally, Al (ca. 80 nm) were thermally deposited. The current density-voltage (*J-V*) curves were measured in a nitrogen glove box and were conducted on a computer-controlled Keithley 2400 source measure unit. Solar cell devices measurement was carried out under AM 1.5G simulated solar illumination (AAA grade, XES-70S1) with the intensity of 100 mW cm^{-2}, reference to standard silicon cell.

3. Measurements of the hole and electron mobility by the space-charge limited current (SCLC) method.

The hole-only or electron-only devices were fabricated using the following architectures: ITO/PEDOT: PSS/active layer/Au for holes and ITO/ titanium (diisopropoxide) bis(2,4-pentanedionate) (TIPD) /active layer/PDINO/Al for electrons. The mobility was extracted by fitting the current density-voltage curves using the Mott-Gurney relationship: $J = 9\varepsilon_0\varepsilon_r\mu V^2/8L^3$ (space-charge limited current), where J is the current density, L is the film thickness of the active layer, μ is the mobility of charge carrier in zero-field, where ε_0 *and* ε_r are the dielectric constant of the films, and $V = V_{\mathrm{app}} - V_{\mathrm{bi}}$, here V_{app} is the applied potential, and V_{bi} is the built-in potential which results from the difference in the work function values of the anode and the cathode. The mobility of charge carriers can be calculated from the slope of the $J^{1/2} \sim V$ curves.

4. Organic synthesis

Synthesis of **ASiBDT-TT**:

^{1}H NMR (400 MHz, CD_2Cl_2) δ ppm: 8.05 (s, 2H), 7.60 (d, *J* = 5.4 Hz, 2H), 7.36 (d, *J* = 5.3 Hz, 2H), 4.41 (q, *J* = 7.1 Hz, 8H), 1.44 (s, 4H), 1.29 (dd, *J* = 18.0, 10.9 Hz, 10H), 1.16 (t, *J* = 7.1 Hz, 42H). ^{13}C NMR (101 MHz, $CDCl_3$) δ 161.93, 143.70, 141.94, 141.43, 138.65, 136.86, 129.90, 125.35, 122.11, 118.77, 111.94, 102.78, 102.09, 77.27, 77.01, 76.69, 61.39, 29.70, 18.79, 14.17, 11.33. TOF-MS (MALDI-TOF) Calcd for $C_{50}H_{58}O_4S_6Si_2$ (M^+): 970.22, Found: 970.1.

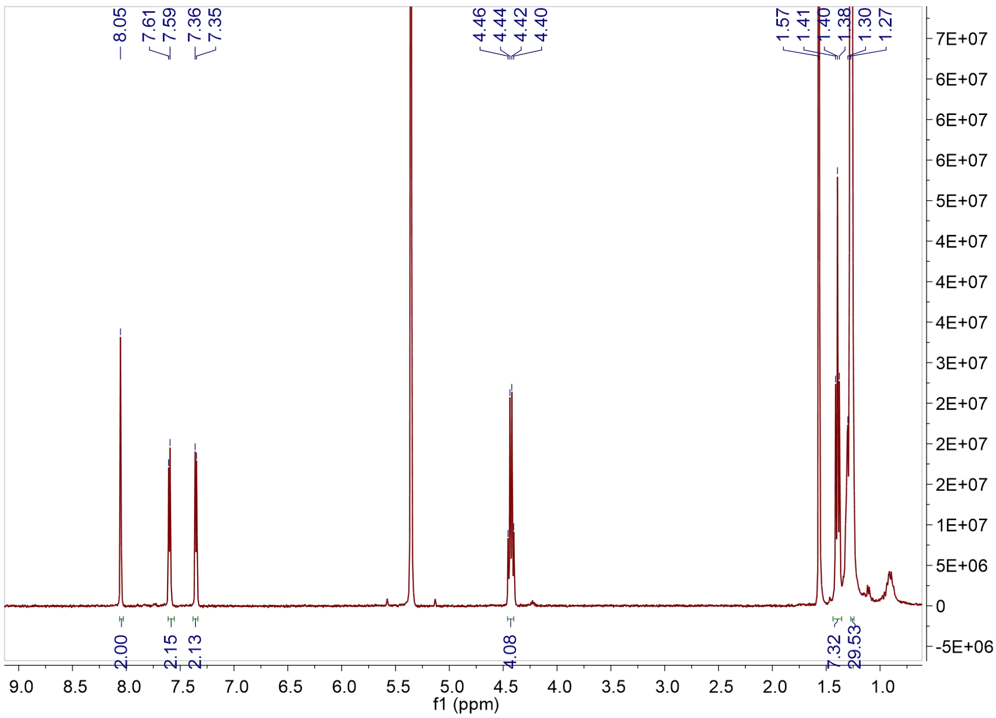

[1]H NMR spectrum of compound ASiBDT-TT

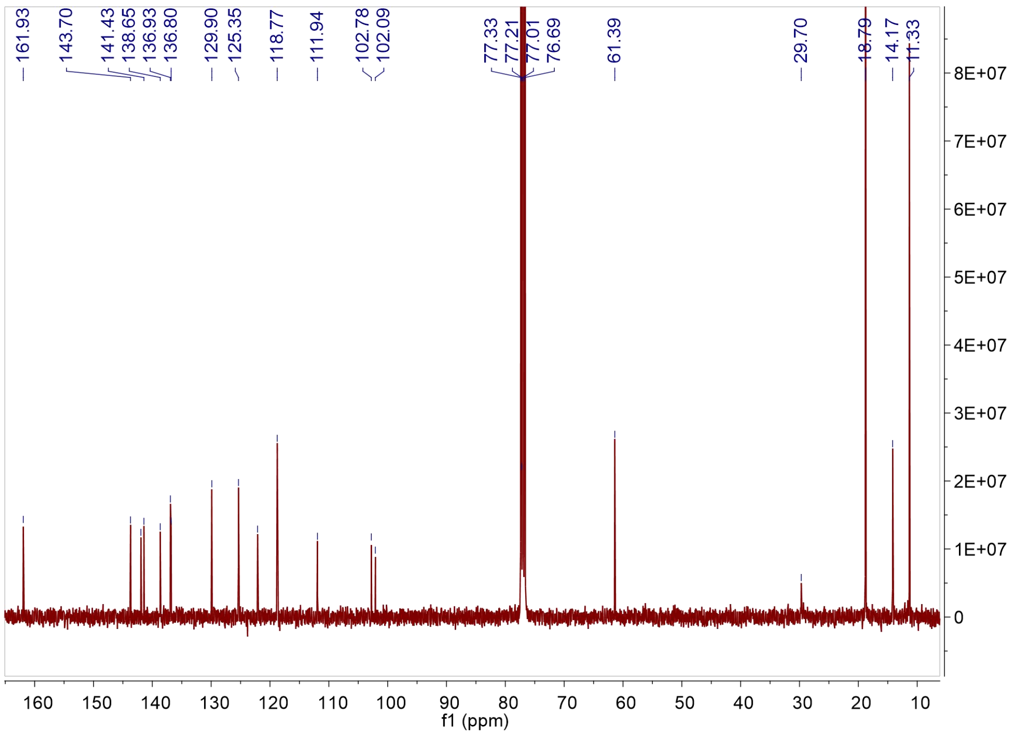

[13]C NMR spectrum of compound ASiBDT-TT

Synthesis of **ASiBDT-2OH**:

^{1}H NMR (400 MHz, $CDCl_3$) δ ppm: δ 7.24 (d, *J* = 5.3 Hz, 2H), 7.18 (s, 2H), 7.15 – 7.09 (m,10H), 6.92 (s, 2H), 6.87 (d, *J* = 8.1 Hz, 8H), 3.12 (s, 2H), 2.32 (t, *J* = 7.7 Hz, 8H), 1.35 (s, 2H), 1.25 (d, *J*

= 5.6 Hz, 8H), 1.16 (d, J = 18.6 Hz, 44H), 1.09 (s, 46H), 0.78 (t, J = 6.7 Hz, 22H). TOF-MS (MALDI-TOF) Calcd for $C_{102}H_{134}O_2S_6Si_2$ (M^+): 1640.72, Found: 1638.82.

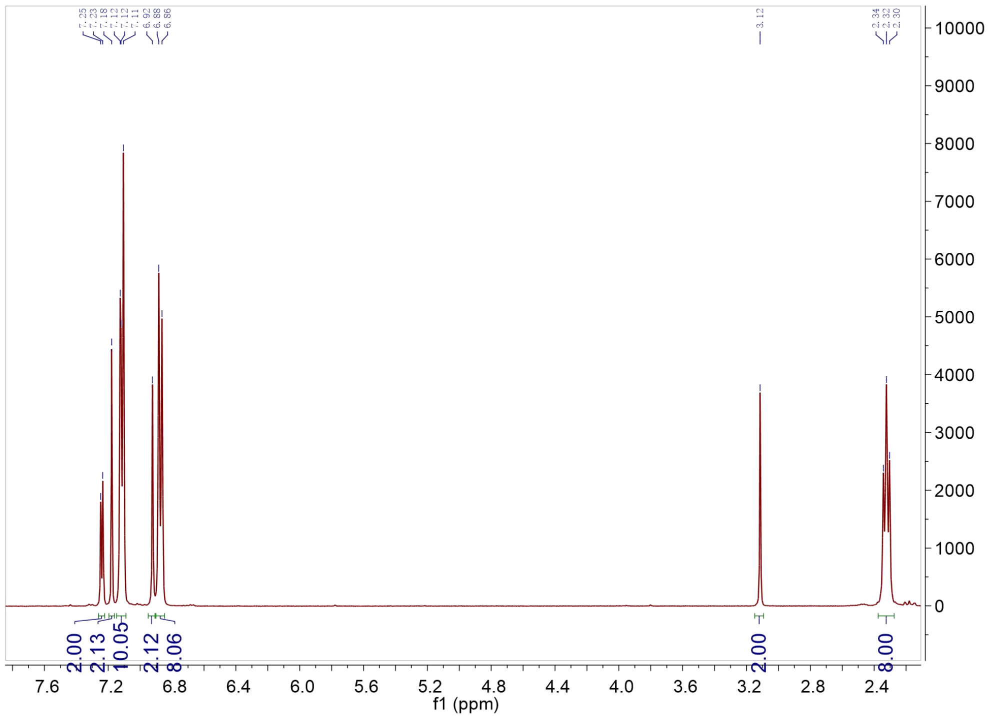

^{1}H NMR spectrum of compound ASiBDT-2OH

Synthesis of **ASiBDTTT**:

^{1}H NMR (300 MHz, $CDCl_3$) ppm: δ 7.50 (d, J = 7.9 Hz, 8H), 7.27 (s, 4H), 7.00 (d, J = 7.9 Hz, 8H), 2.47 (t, J = 7.7 Hz, 8H), 1.57 (d, J = 5.2 Hz, 8H), 1.28 (s, 44H), 1.10 (s, 44H), 0.90 (t, J = 6.3 Hz, 16H). TOF-MS (MALDI-TOF) Calcd for $C_{102}H_{130}O_2S_6Si_2$ (M^+): 1604.70, Found: 1602.80.

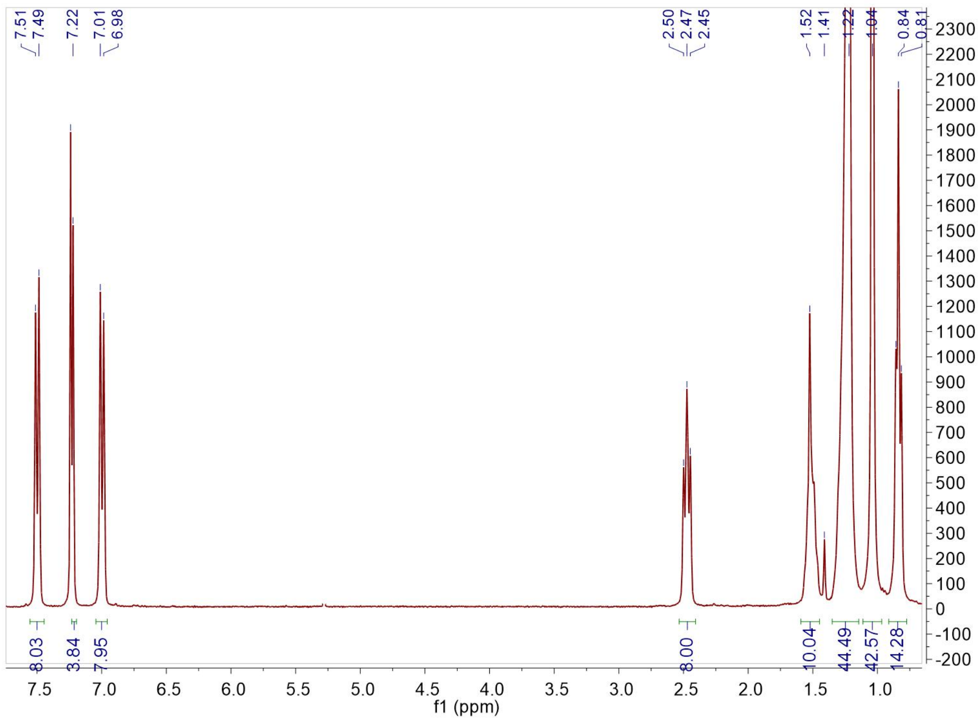

[1]H NMR spectrum of compound SiBDTTT

Synthesis of **ASiBDTTT-2CHO**:

^{1}H NMR (400 MHz, CD_2Cl_2) δ ppm: 9.78 (s, 2H), 7.87 (s, 2H), 7.42 (d, *J* = 8.1 Hz, 8H), 6.98 (d, *J* = 8.1 Hz, 8H), 2.50 – 2.37 (m, 8H), 1.45 (s, 16H), 1.17 (d, *J* = 11.9 Hz, 44H), 0.98 (s, 40H), 0.77 (t, *J* = 6.5 Hz, 12H). ^{13}C NMR (101 MHz, $CDCl_3$) δ 182.75, 153.34, 152.35, 151.30, 143.81, 143.29, 142.15, 141.70, 140.66, 139.97, 135.11, 130.25, 129.53, 128.74, 128.46, 113.28, 107.75, 104.47, 77.27, 77.01, 76.69, 64.69, 35.57, 31.86, 31.09, 29.52, 29.21, 22.65, 18.86, 14.08, 11.79. (MALDI-TOF) Calcd for $C_{104}H_{130}O_2S_6Si_2$ (M^+): 1658.79. Found: 1659.5.

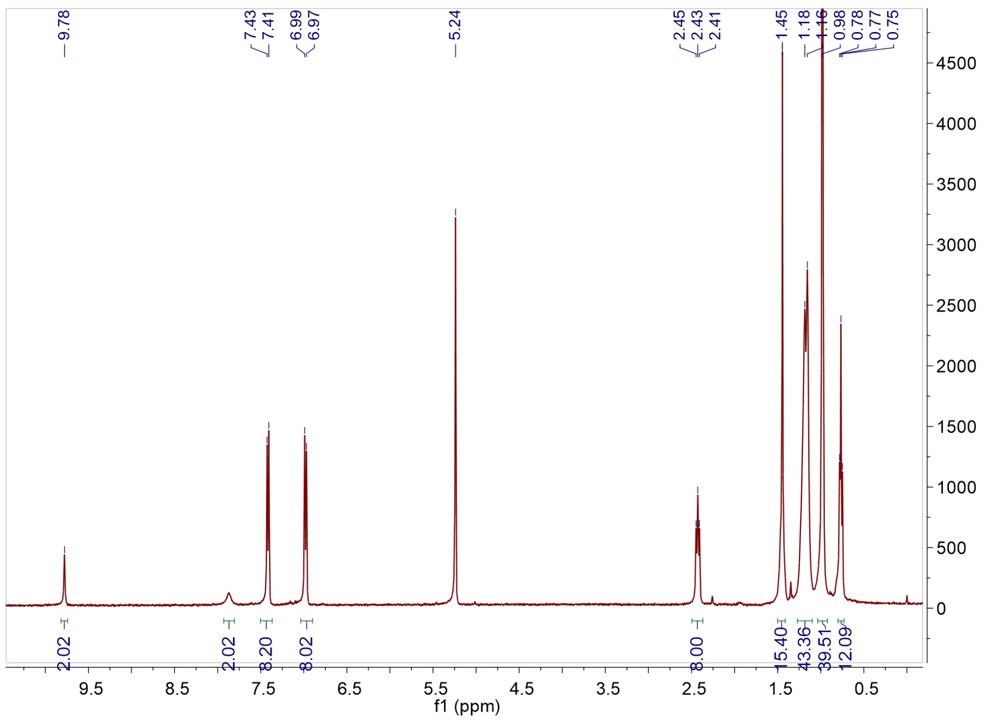

^{1}H NMR spectrum of compound ASiBDTTT-2CHO

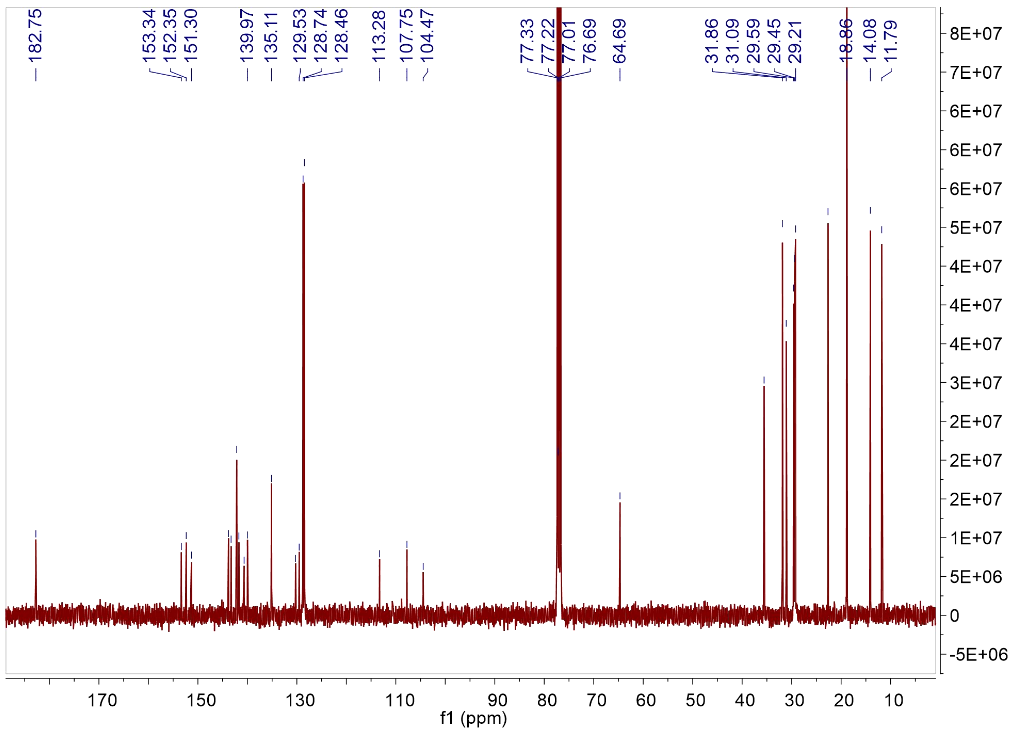

^{13}C NMR spectrum of compound ASiBDTTT-2CHO

Synthesis of **ISI-4F/Cl:**

^{1}H NMR (300 MHz, $CDCl_3$) δ 8.84 (s, 2H), 8.60 – 8.52 (m, 2H), 8.21 (s, 2H), 7.74 (t, *J* = 7.5 Hz, 2H), 7.57 (d, *J* = 7.8 Hz, 8H), 7.11 (d, *J* = 8.0 Hz, 8H), 2.62 – 2.44 (m, 8H), 1.58 (s, 18H), 1.24 (s, 38H), 1.10 (s, 38H), 0.85 (t, *J* = 6.0 Hz, 12H). ^{13}C NMR (101 MHz, $CDCl_3$) δ 185.75, 158.21, 155.40, 155.05, 154.40, 152.13, 147.79, 147.23, 143.88, 142.39, 141.03, 139.46, 139.01, 138.58, 137.20, 134.69, 130.37, 128.72, 121.55, 115.07, 114.25, 113.77, 112.52, 108.77, 104.29, 77.28, 77.02, 76.70, 69.55, 64.84, 35.58, 31.86, 31.06, 29.52, 29.22, 22.64, 18.89, 14.07, 11.82. TOF-MS (MALDI-TOF) Calcd for $C_{128}H_{134}F_4N_4O_2S_6Si_2$ (M^+): 2082.83, Found: 2083.5.

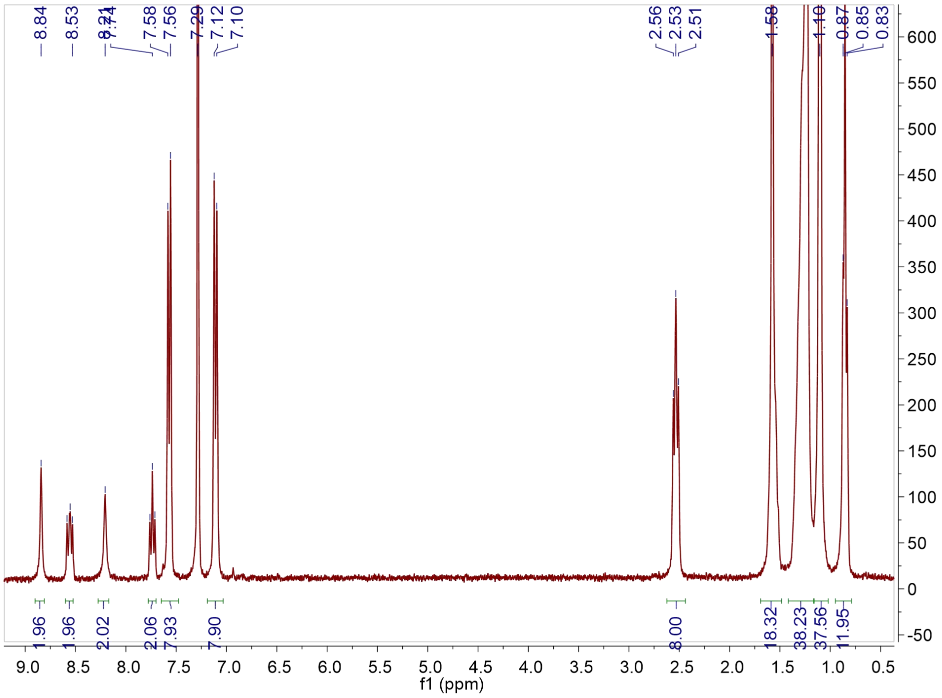

[1]H NMR spectrum of compound ISI-4F

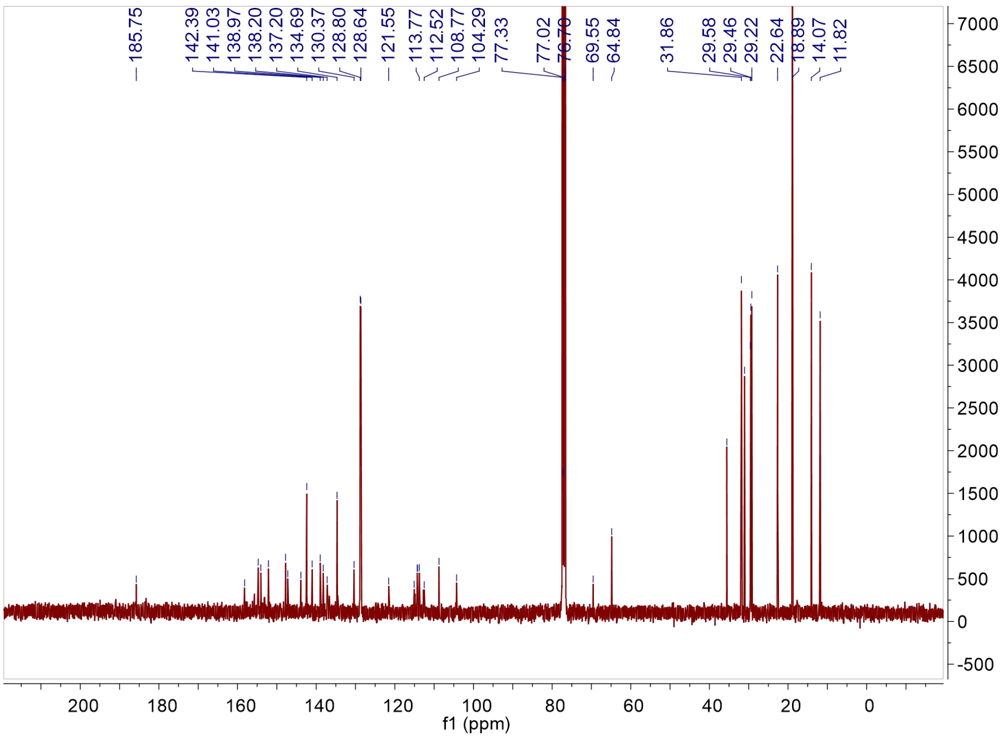

[13]C NMR spectrum of compound ISI-4F

^1H NMR (400 MHz, $CDCl_3$) δ 8.77 (s, 2H), 8.69 (s, 2H), 8.11 (s, 2H), 7.91 (s, 2H), 7.47 (d, J = 8.1 Hz, 8H), 7.02 (d, J = 8.2 Hz, 8H), 2.51 – 2.39 (m, 8H), 1.18 (t, J = 16.7 Hz, 54H), 1.01 (s, 40H), 0.77 (dd, J = 16.9, 10.8 Hz, 18H). ^{13}C NMR (101 MHz, $CDCl_3$) δ 185.75, 158.21, 154.90, 152.17, 148.13, 142.41, 141.07, 139.70, 139.38, 138.69, 135.99, 134.62, 130.39, 128.79, 128.79, 128.65, 126.92, 125.17, 121.50, 114.29, 11281, 108.38, 104.25, 69.58, 64.82, 35.57, 31.86, 31.06, 29.57, 29.46, 29.22, 22.65, 18.80, 14.07, 11.82. TOF-MS (MALDI-TOF) Calcd for $C_{128}H_{134}Cl_4N_4O_2S_6Si_2$ (M^+): 2148.71, Found: 2149.4.

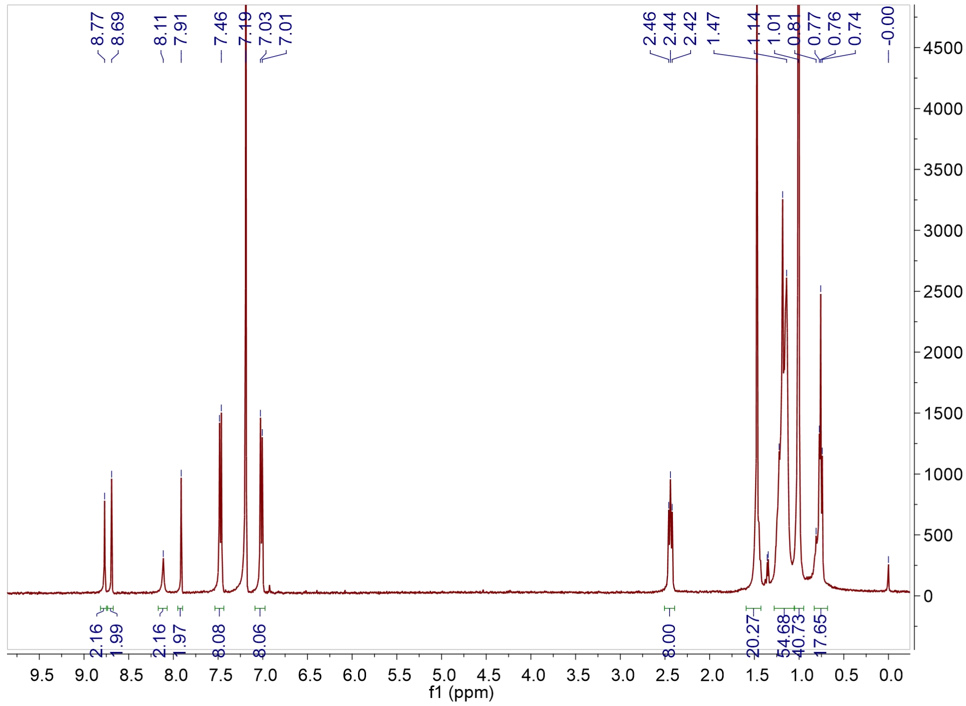

^1H NMR spectrum of compound ISI-4Cl

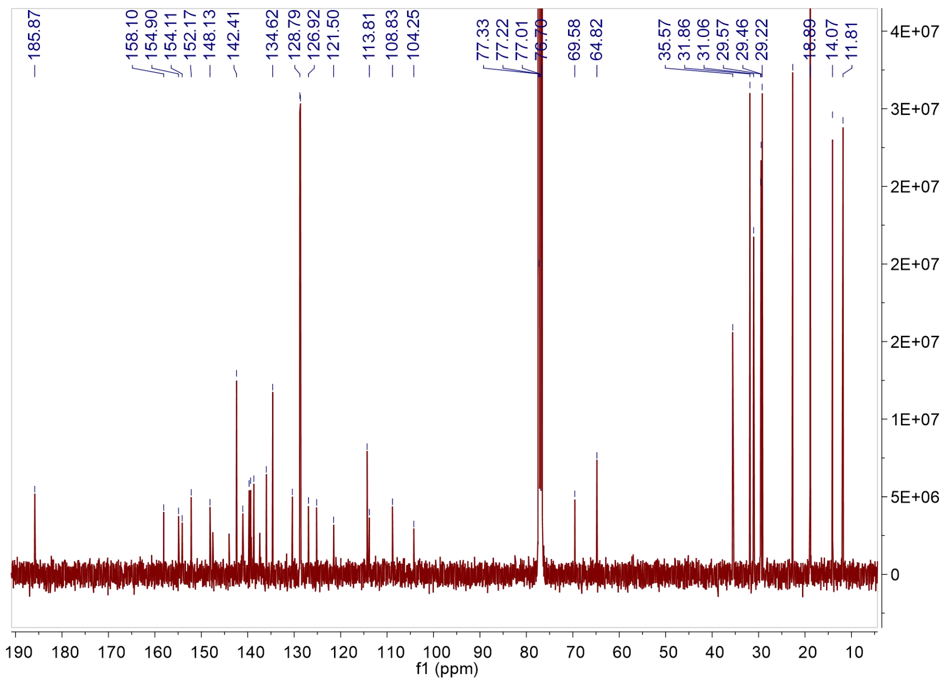

^{13}C NMR spectrum of compound ISI-4Cl

5. Supporting figures and tables for Thermal, optical and photovoltaic data

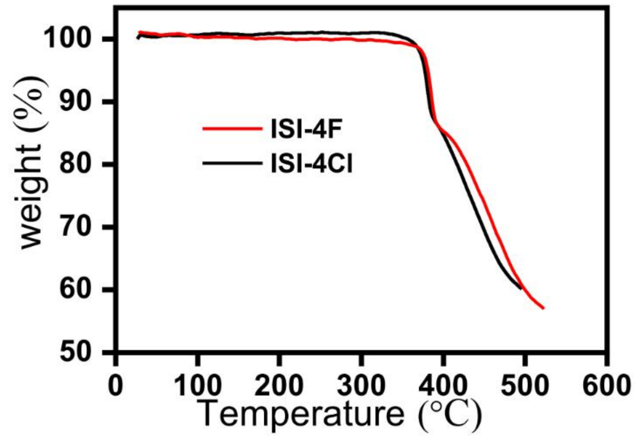

Figure S1. Thermogravimetric analysis (TGA) plots of ISI-4F and ISI-4Cl.

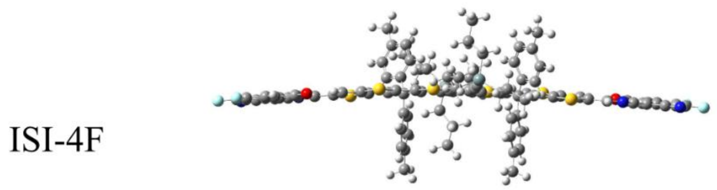

Figure S2. The optimized molecular conformations of ISI-4F and ISI-4Cl.

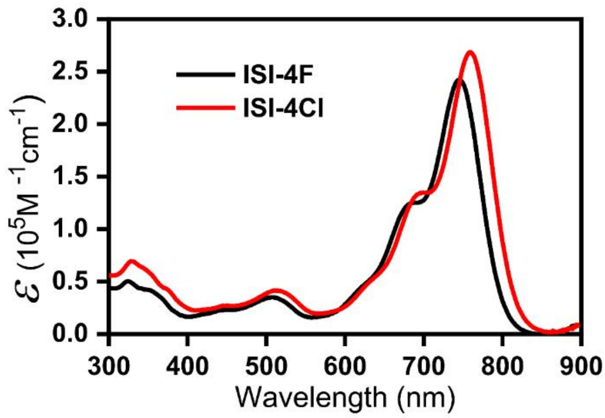

Figure S3. The absorption spectra of ISI-4F, ISI-4Cl in diluted chloroform solution.

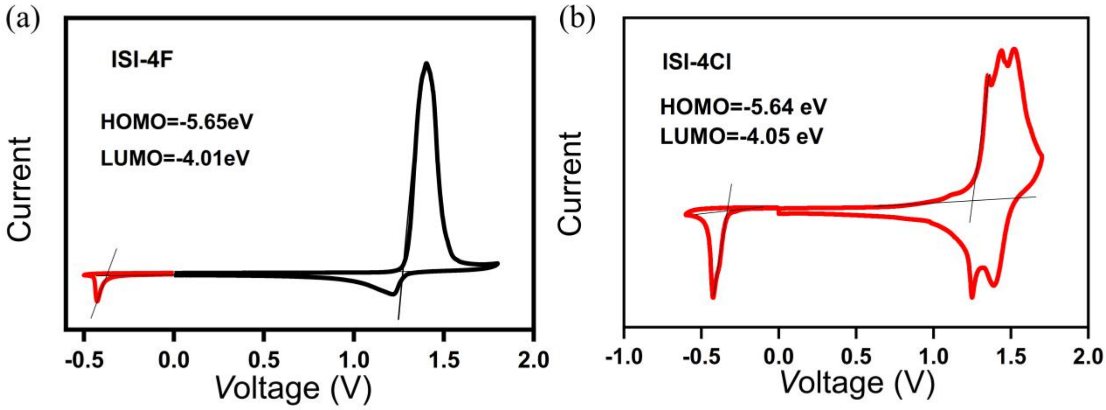

Figure S4. The cycle voltammetry (CV) curves of (a) ISI-4F and (b) ISI-4Cl pure films measured in an N_2-degassed anhydrous CH_3CN solution, respectively.

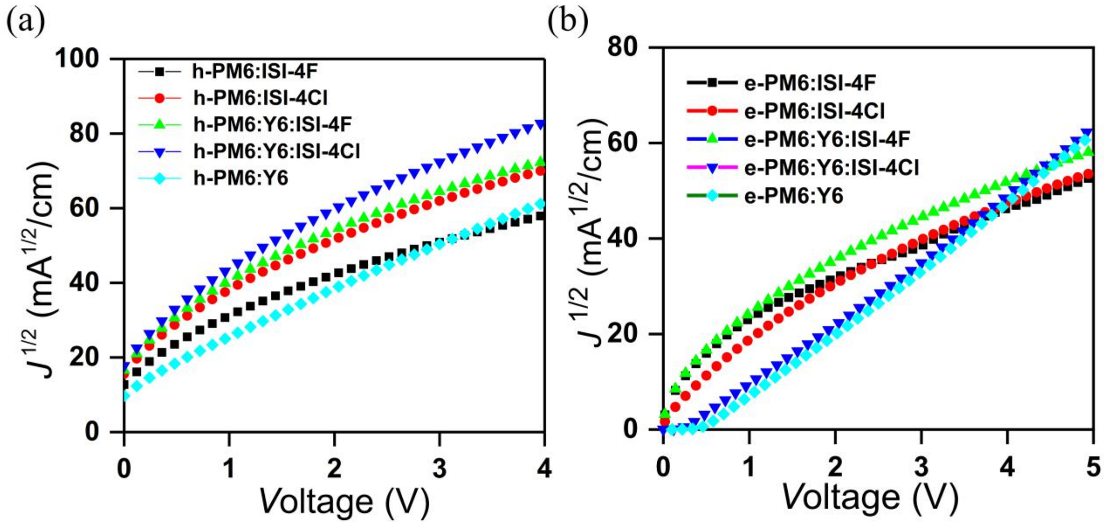

Figure S5. The plots of $J^{1/2}$ *vs.* Voltage for calculations of (a) electron and (b) hole mobilities.

Table S1. The photovoltaic data of binary solar cells with different proportion of additives chloronaphthalene (CN).

Active layer	CN (%)	V_{OC} (V)	J_{SC} (mA/cm^2)	FF (%)	PCE (%)
PM6:ISI-4F	0	0.913	19.6	50.67	9.1
	0.25	0.910	17.5	61.70	9.8
	0.5	0.902	20.4	58.58	10.8
	0.75	0.904	21.2	59.63	11.4
	1.0	0.893	21.2	62.94	11.9
	1.2	0.896	20.8	59.99	11.2
PM6:ISI-4Cl	0	0.833	22.7	54.34	10.2
	0.25	0.882	22.0	49.64	9.6
	0.5	0.859	20.2	60.77	10.5
	0.75	0.861	20.5	67.55	11.9
	1.0	0.870	20.2	65.86	11.6

Table S2. Values of the electron and the hole and their ratios of the ISI-4F, ISI-4Cl, IN-4F and Y6 based binary and ternary solar cell blended films.

Active layer	μ_h (10^{-4} cm^2 V^{-1} s^{-1})	μ_e (10^{-4} cm^2 V^{-1} s^{-1})	μ_h/μ_e
PM6:ISI-4F	2.2	4.3	0.51
PM6:ISI-4Cl	2.3	3.2	0.70
PM6:IN-4F	7.3	6.8	1.07
PM6:Y6	2.8	3.2	0.88
PM6:Y6:IN-4F	3.5	5.5	0.63
PM6:Y6:ISI-4F	4.4	3.4	1.29
PM6:Y6:ISI-4Cl	4.3	3.3	1.30

Table S3. Values of α, n and $J_{ph,sc}$, $J_{ph,sat}$ and $J_{ph,sc}/J_{ph,sat}$ for the optimal binary, ternary blended films based on ISI-4F and ISI-4Cl.

Active layer	α	n	$J_{ph,sc}$ (mAcm^{-2})	$J_{ph,sat}$ (mAcm^{-2})	$J_{ph,sc}/J_{ph,sat}$
PM6:ISI-4F	0.988	1.15	22.4	24.2	92.6%
PM6:ISI-4Cl	0.983	1.19	20.9	22.2	94.1%
PM6:Y6:ISI-4F	0.989	1.12	25.4	26.1	97.3%
PM6:Y6:ISI-4Cl	0.989	1.14	25.7	26.5	97.0%
PM6:Y6	0.986	1.22	25.0	25.5	98.0%

Table S4. The photovoltaic data of ternary solar cells with different mass ratios of ISI-4F and ISI-4Cl.

	X	V_{OC} (V)	J_{SC} (mA/cm^2)	FF (%)	PCE (%)
PM6:Y6:ISI-4F=1:1.2:X	0.1	0.844	25.7	74.21	16.1
	0.2	0.839	25.2	73.40	15.6
PM6:Y6:ISI-4Cl=1:1.2:X	0.1	0.847	25.3	74.14	15.9
	0.2	0.842	25.3	72.50	15.4